author: Ocean Wong
date: April 2025
Organization: Culham Centre for Fusion Energy

Abstract

To calculate crude approximations of the neutron flux(es) in the first wall and blanket of a fusion reactor in a reactor-design-agnostic manner, a semi-infinite model of the fusion neutron source, first-wall, and blanket are created. The one-group neutron transport equation is solved analytically while the multi-group neutron transport equation is solved numerically.

Keywords: semi-infinite slab, fusion neutronics

1 Simplification of the PROCESS model

We would like to implement an elementary way of approximating the number of neutrons passing through and absorbed by the first wall and blanket of a fusion reactor in the reactor systems code PROCESS. Since most of PROCESS's plasma simulation models uses 1D model, with "radial distance from the center of the plasma" as the only coordinate, it is sensible to follow the same convention when performing our neutronics calculation, and assume that we are working with a cylindrical model (Figure 1).

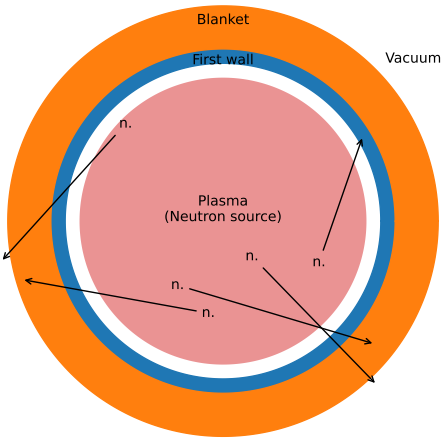

Figure 1: The x-z cross-section of an example neutronics model appropriate for PROCESS.

Solving the neutron flux on this model using Equation 3 would yield a sum involving Airy functions, which is a complex function not typically found in numerical solver packages. Therefore, we choose to further simplify the geometry represented by Figure 1. By taking a horizontal slice of the figure at the plane of symmetry, we get:

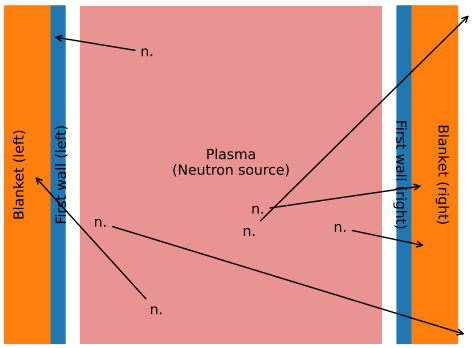

Figure 2: A simple x cross-section of the an example neutronics model appropriate for PROCESS, obtained by taking a horiztonal slice of Figure 1.

Since the plasma only acts as a neutrons source, and is otherwise transparent to neutrons (i.e. neutrons passing through the plasma do not change direction), we can collapse the space between the left and right first wall, and approximate the plasma neutron source as a planar source instead (Figure 3):

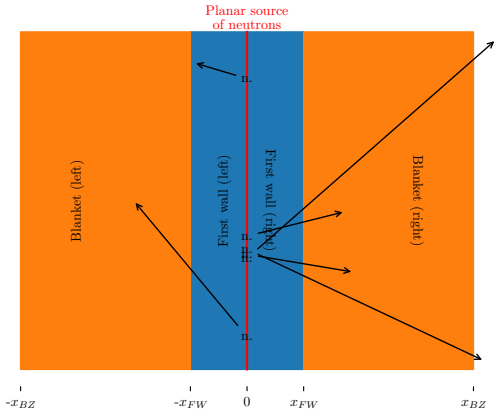

Figure 3: A simple x cross-section of the an example neutronics model appropriate for PROCESS, obtained by collapsing the neutron-transparent space in Figure 2. The blanket and first wall extends infinitely in the other two directions, i.e. vertically (up/down) and in/out of the page.

Thus figure 3 represent a semi-infinite slab (finite thickness in the x-direction, but extends infinitely in the y- and z-directions).

The neutron transport equation is given by [1] in full as:

$$\underbrace{\frac{1}{v}\frac{d\phi}{dt}}_{\text{time-dependence}} + \underbrace{\hat{\boldsymbol{\Omega}} \cdot \boldsymbol{\nabla}\phi}_{\text{streaming}} + \underbrace{\Sigma_t \phi}_{\text{collision/removal}} = \underbrace{\Sigma_s \phi}_{\text{scattering-in from other energy groups}} + \underbrace{\boldsymbol{S}}_{\text{other sources}} . \quad (1)$$

All terms in Equation 1 are implicitly dependent on angle ($\boldsymbol{\Omega}$), neutron energy, position ($\boldsymbol{r}$), and time.

2 Simplification of the neutron transport equation

Some of the variables are explained below:

- Σ_t = total macroscopic cross-section
- Σ_s = (elastic) scattering macroscopic cross-section
- Σ_i = macroscopic cross-section of reaction $i = n_d\sigma_i$ = number density × microscopic cross-section of reaction i. Number density can be obtained by $N_d = \frac{N_A}{A}\rho = \frac{\text{Avogadro's number}}{\text{atomic number}} \times$ density.

We also make the assumption that all neutron reactions that aren't elastically scattered are considered absorbed/lost due to transmutation, and that the fraction of atoms transmuted is insignificant for changing the neutronics properties of the material.

Duderstadt and Hamilton made several simplifications that makes Equation 1 soluble.

2.1 Removing time-dependence and fission sources

The assumption of steady state operation and lack of fission sources in the media removes the leftmost and rightmost terms in Equation 1, giving:

$$\hat{\boldsymbol{\Omega}} \cdot \boldsymbol{\nabla}\phi + \Sigma_t\phi = \Sigma_s\phi\,, \tag{2}$$

ϕ is now only implicitly dependent on angle ($\boldsymbol{\Omega}$), neutron energy, and position ($\boldsymbol{r}$); but is time-invariant.

2.2 Simplifying the streaming term

Then, to turn the streaming term into something manageable, the neutron flux is assumed to be isotropic everywhere. This is not entirely true in our case, where the neutron emitted from the plasma monoenergetic neutron source is assumed to be a narrow band of 14.1 MeV neutrons, such that neutrons streaming in the horizontal direction (perpendicular to the plane source in Figure 3) will preferentially travel further, meaning that, far away from the neutron source, the distribution of neutron directions forms a spike pointed to the left/right, rather than a spherical cloud. However, this is deemed as an acceptable simplification required to proceed with the derivation. This converts the "neutron transport equation" into a "neutron diffusion equation":

$$-D\boldsymbol{\nabla}^2\phi + \Sigma_t\phi = \Sigma_s\phi\,. \tag{3}$$

Note that the neutron flux profiles generated by solving Equation 3 differs from the neutron flux profile generated by solving Equation 1 near locations of abrupt changes, such as within several λ_{tr} around the plane source or the vacuum boundary. However, this difference is only minute, as stated in p.159-160 of [1].

The left most term is described as the Fick's Law term due to its visual similarity to the Fick's Law of Diffusion, despite its diffusion coefficient D (defined in Section 2.3) having a different dimensionality (length) than when it appears in other fields of physics (area per unit time).

2.3 Discretizing into energy groups

The final step is to discretize the neutron spectrum into different energy groups, such that for each group's flux ϕ_i, Σ_t and Σ_s are scalars, rather than functions requiring interpolation. (Note that ϕ_i is still implicitly dependent on position $\boldsymbol{r}$.) The larger the group number i, the higher the neutron lethargy, i.e. the less energy it has. (Remember that neutron lethargy is defined as $ln(\frac{E_0}{E})$, where E_0 is the initial energy of the neutron at its creation).

Assuming that neutrons can only downscatter (i.e. neutron energy $\gg$ thermal energy of the medium), we only have to sum up[1] all of the scattered-in neutrons from higher energy neutrons.

$$-D\boldsymbol{\nabla}^2\phi_i + \Sigma_t\phi_i = \sum_{j}^{j\leq i} \Sigma_{s(i\to j)}\phi_j \,. \tag{4}$$

The diffusion coefficient D is given by p.136 of [1] as:

$$D = \frac{1}{3\Sigma_{tr}} = \frac{\lambda_{tr}}{3} = \frac{1}{3(\Sigma_t - \frac{2}{3A}\Sigma_s)} \,, \tag{5}$$

where

- A is, as mentioned above, the atomic number of the medium being travelled through by the neutrons;
- λ_{tr} is known as the mean-free-path of neutrons (for the given energy group and medium);
- $\Sigma_s \equiv \Sigma_{s,(i\to i)}$ is scattering cross-sections from the current group i back into the current group i.

For the one group analysis, we omit the group number subscript, e.g. the $(1 \to 1)$ subscript of Σ_s is omitted.

2.4 Taking advantage of the symmetry in the y- and z-direction

Finally, we can remove the dependence on the other two spatial dimension, such that the diffusion equation can be simplified as:

$$-D\frac{d^2}{dx^2}\phi_i(x) + \Sigma_t\phi_i(x) = \sum_{j}^{j\leq i} \Sigma_{s(i\to j)}\phi_j(x) \tag{6}$$

$$D\frac{d^2}{dx^2}\phi_i(x) = \Sigma_t\phi_i(x) - \sum_{j}^{j\leq i} \Sigma_{s(i\to j)}\phi_j(x) \,. \tag{7}$$

Now that the spatial dependence is more explicitly written ($\phi_i(x)$), we can begin solving for the solution.

3 One-group solution

This section's content is similar to the derivation on p.163-164, but the boundary conditions are different, hence a different result is produced.

[1] Beware of confusion between summation sign $\sum$ and the macroscopic-cross-section sign Σ. It should be easy to tell them apart from context.

If we assume the cross-sections for scattering and other reactions remains constant throughout the entire neutron spectrum, then we can re-use the same scalar values of Σ_t and Σ_s for all of the neutrons. Considering that we are evaluating the neutron flux emitted at $x = 0$, propagating left and right into a purely-absorbing (i.e. non-fissile) medium (refer to Figure 3), it is intuitive that the solution is some form of exponential decay on both sides of the source, where the neutron flux the further it travels into the first wall and blanket. And indeed, by applying the appropriate boundary conditions, we can obtain that result.

Let the incident neutron flux on the first wall be $\boldsymbol{f}$ (SI unit: $\mathrm{m}^{-2}\mathrm{s}^{-1}$). Examining only the right-hand-side (i.e. $x > 0$) of the model, we can derive the following:

$$D\frac{d^2}{dx^2}\phi(x) = (\Sigma_t - \Sigma_s)\phi(x)\,, \tag{8}$$

Solving this equation can be made easier if we first define a variable named L.

$$\begin{aligned} L^2 &= \frac{D}{\Sigma_t - \Sigma_s} \\ L &= \sqrt{\frac{D}{\Sigma_t - \Sigma_s}}\,. \end{aligned} \tag{9}$$

For the one group case ($i = 1$ only), $\Sigma_s \equiv \Sigma_{s(1\to1)}$. Note that the diffusion coefficient D and macroscopic cross-sections Σ_s and Σ_t are going to be different in the first wall v.s. in the blanket, hence there are two different D, denoted D_{FW} and D_{BZ}, and correspondingly, L becomes L_{FW} and L_{BZ} respectively.

Let's express the thickness of the first wall and thickness of the blanket as "first wall thickness" $= x_{FW}$, "blanket thickness" $= x_{BZ} - x_{FW}$, such that the interface between the blanket and the vacuum boundary is located at x_{BZ}, as denoted in Figure 3.

Solving Equation 8 then gives the following two piecewise functions:

$$\phi(x) = \begin{cases} c_1 e^{\frac{|x|}{L_{FW}}} + c_2 e^{-\frac{|x|}{L_{FW}}} & \text{when} \quad 0 < |x| \le x_{FW}\,, \\ c_3 e^{\frac{|x|}{L_{BZ}}} + c_4 e^{-\frac{|x|}{L_{BZ}}} & \text{when } x_{FW} < |x| \le x_{BZ} + \delta\,. \end{cases} \tag{10}$$

c_1, c_2, c_3, c_4 are all integration constants to be determined using the boundary conditions in Section 3.1. An extrapolation length of $\delta = 0.7104\,\lambda_{tr} = 0.7104 \times 3D_{BZ}$ is added onto the vacuum boundary to obtain a more realistic flux profile, to counteract the inaccuracy introduced by approximating the transport equation with a diffusion equation. The details of this deviation, and the why extending the vacuum boundary like such makes the diffusion approximation valid again, is explained in p.144 of [1].

3.1 Boundary conditions

- Neutron current density seeping out of either side of the plane source is equal to the incident neutron flux on the first wall, i.e.

$$\begin{aligned} \boldsymbol{J}_x(0^+) &= \boldsymbol{f} \\ -D\frac{d}{dx}\phi(x)\bigg|_{x=0^+} &= \boldsymbol{f}\,, \end{aligned} \tag{11}$$

  for group 1 neutrons (i.e. neutrons in the same energy group as the source neutrons).

- Flux continuity at the first-wall-blanket interface x_{FW}, i.e.

$$\phi(x_{FW} - \varepsilon) = \phi(x_{FW} + \varepsilon) \tag{12}$$

or more formally,

$$\lim_{\varepsilon \to 0}(\phi(x_{FW} - \varepsilon) - \phi(x_{FW} + \varepsilon)) = 0\,.$$

- Since the flux on either side of the first-wall-blanket interface is stable (i.e. time-invariant), the neutron current density from first wall to blanket = neutron current density from blanket to first wall at the interface x_{FW}, i.e.

$$\begin{aligned} \boldsymbol{J}_x(x_{FW} - \varepsilon) &= \boldsymbol{J}_x(x_{FW} + \varepsilon) \\ -D_{FW}\frac{d}{dx}\phi(x)\bigg|_{x_{FW}-\varepsilon} &= -D_{BZ}\frac{d}{dx}\phi(x)\bigg|_{x_{FW}+\varepsilon} \\ D_{FW}\frac{d}{dx}\phi(x)\bigg|_{x_{FW}-\varepsilon} &= D_{BZ}\frac{d}{dx}\phi(x)\bigg|_{x_{FW}+\varepsilon} \end{aligned} \tag{13}$$

or more formally,

$$\lim_{\varepsilon \to 0}\left(D_{FW}\frac{d}{dx}\phi(x)\bigg|_{x_{FW}-\varepsilon} - D_{BZ}\frac{d}{dx}\phi(x)\bigg|_{x_{FW}+\varepsilon}\right) = 0$$

- The flux is expected to drop to zero at the *extended boundary*, i.e.

$$\phi(x_{BZ} + \delta) = 0 \tag{14}$$

After a somewhat-intensive evaluation of simultaneous Equations 11, 12, 13, and 14, we have:

$$c_2 = \left(\frac{\boldsymbol{f}}{2}\right) \cdot e^{\frac{x_{FW}}{L_{FW}}} \frac{\frac{L_{FW}}{D_{FW}} + \frac{L_{BZ}}{D_{BZ}}\tanh\left(\frac{x_{BZ}+\delta-x_{FW}}{L_{BZ}}\right)}{\cosh\left(\frac{x_{FW}}{L_{FW}}\right) + \sinh\left(\frac{x_{FW}}{L_{FW}}\right)\tanh\left(\frac{x_{BZ}+\delta-x_{FW}}{L_{BZ}}\right)\frac{D_{FW}}{L_{FW}}\frac{L_{BZ}}{D_{BZ}}} \tag{15}$$

$$c_1 = c_2 - \frac{L_{FW}}{D_{FW}}\boldsymbol{f} \tag{16}$$

$$c_4 = \left(\frac{\boldsymbol{f}}{2}\frac{L_{FW}}{D_{FW}}e^{\frac{x_{FW}}{L_{FW}}}\right) \cdot e^{\frac{x_{BZ}+\delta}{L_{BZ}}} \frac{1 - \tanh\left(\frac{x_{FW}}{L_{FW}}\right)}{\frac{D_{BZ}}{L_{BZ}}\frac{L_{FW}}{D_{FW}}\cosh\left(\frac{x_{BZ}+\delta-x_{FW}}{L_{BZ}}\right) + \tanh\left(\frac{x_{FW}}{L_{FW}}\right)\sinh\left(\frac{x_{BZ}+\delta-x_{FW}}{L_{BZ}}\right)} \tag{17}$$

$$\begin{aligned} c_3 &= -c_4 e^{-\frac{2(x_{BZ}+\delta)}{L_{BZ}}} \\ &= \left(-\frac{\boldsymbol{f}}{2}\frac{L_{FW}}{D_{FW}}e^{\frac{x_{FW}}{L_{FW}}}\right) \cdot e^{-\frac{x_{BZ}+\delta}{L_{BZ}}} \frac{1 - \tanh\left(\frac{x_{FW}}{L_{FW}}\right)}{\frac{D_{BZ}}{L_{BZ}}\frac{L_{FW}}{D_{FW}}\cosh\left(\frac{x_{BZ}+\delta-x_{FW}}{L_{BZ}}\right) + \tanh\left(\frac{x_{FW}}{L_{FW}}\right)\sinh\left(\frac{x_{BZ}+\delta-x_{FW}}{L_{BZ}}\right)} \end{aligned} \tag{18}$$

Finally, this yields a flux profile as shown in Figure 4. To see the effect of changing different parameters interactively, please use the Desmos link `https://www.desmos.com/calculator/18xojespuo`.

Combining Equation 10 and the constants in Equations 15 to 17, the neutron flux at any depth $|x| < x_{BZ}, x \neq 0$ can be predicted.

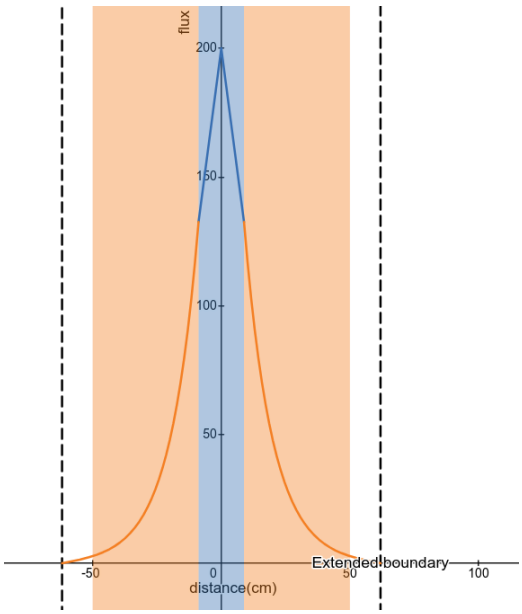

(a) The case where the total macroscopic cross-section of the blanket is greater than that of the first wall.

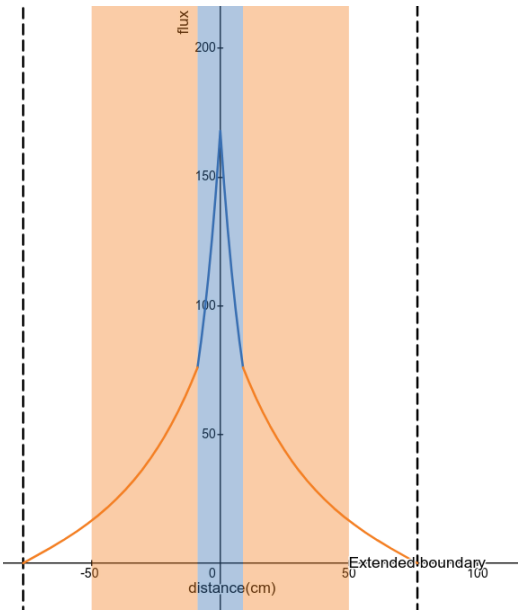

(b) The case where the total macroscopic cross-section of the first wall is greater than that of the blanket.

Figure 4: Examples of the neutron flux profiles predicted by the neutron diffusion equation using the one-group model under a variety of combination of cross-section ratios.

3.2 Rates

The average number of neutron-induced reactions per unit volume between the depths $x = a$ to $x = b$,

$$\text{reaction rate} = \int_{x=a}^{x=b} \Sigma\phi(x)dx\,, \tag{19}$$

The indefinite integral is for the first wall region is

$$L_{FW}(c_1 e^{\frac{|x|}{L_{FW}}} - c_2 e^{-\frac{|x|}{L_{FW}}}) + C \tag{20}$$

and for the blanket region is

$$L_{BZ}(c_3 e^{\frac{|x|}{L_{BZ}}} - c_4 e^{-\frac{|x|}{L_{BZ}}}) + C \tag{21}$$

in the blanket region.

We can replace Σ with $(\Sigma_t - \Sigma_s)$ to count only non-scattering reactions, or we can replace it with Σ_t to count all reactions.

For any interface located at position x', we can also calculate the number of neutrons passing through every unit area of this interface using the equation:

$$\text{Neutron escape rate} = -D\frac{d}{dx}\phi(x)\bigg|_{x'} \tag{22}$$

$$\text{rate of neutrons exiting the first wall} = -\frac{D_{FW}}{L_{FW}}\left(c_1 e^{\frac{x_{FW}}{L_{FW}}} - c_2 e^{-\frac{x_{FW}}{L_{FW}}}\right)\,, \tag{23}$$

$$\text{rate of neutrons entering the blanket} = -\frac{D_{BZ}}{L_{BZ}}\left(c_3 e^{\frac{x_{FW}}{L_{BZ}}} - c_4 e^{-\frac{x_{FW}}{L_{BZ}}}\right)\,. \tag{24}$$

The quantity in Equation 22 and 23 should be the same by construction, as enforced by condition 13. Evaluating the latter expression, the net number of neutrons streaming from left to right across the first-wall-blanket interface per unit area

$$\begin{aligned}
&= c_4 \frac{D_{BZ}}{L_{BZ}} e^{-\frac{(x_{BZ}+\delta)}{L_{BZ}}} 2\cosh\left(\frac{x_{BZ}+\delta-x_{FW}}{L_{BZ}}\right) \\
&= \frac{\boldsymbol{f} e^{\frac{x_{FW}}{L_{FW}}}\left(1-\tanh\left(\frac{x_{FW}}{L_{FW}}\right)\right)}{1+\tanh\left(\frac{x_{FW}}{L_{FW}}\right)\tanh\left(\frac{x_{BZ}+\delta-x_{FW}}{L_{BZ}}\right)\frac{D_{FW}}{L_{FW}}\frac{L_{BZ}}{D_{BZ}}} \,.
\end{aligned} \tag{25}$$

As for the number of neutrons escaping the model into the vacuum (void),

$$\begin{aligned}
&\text{rate of neutrons exiting the blanket (lost to the void)} = -\frac{D_{BZ}}{L_{BZ}}\left(c_3 e^{\frac{x_{BZ}}{L_{BZ}}} - c_4 e^{-\frac{x_{BZ}}{L_{BZ}}}\right) \\
&= c_4 \frac{D_{BZ}}{L_{BZ}} e^{-\frac{x_{BZ}+\delta}{L_{BZ}}} 2\cosh\left(\frac{\delta}{L_{BZ}}\right) \\
&= \left(\boldsymbol{f}\frac{L_{FW}}{D_{FW}}\frac{D_{BZ}}{L_{BZ}} e^{\frac{x_{FW}}{L_{FW}}}\right) \frac{\cosh\left(\frac{\delta}{L_{BZ}}\right)\left(1-\tanh\left(\frac{x_{FW}}{L_{FW}}\right)\right)}{\frac{D_{BZ}}{L_{BZ}}\frac{L_{FW}}{D_{FW}}\cosh\left(\frac{x_{BZ}+\delta-x_{FW}}{L_{BZ}}\right)+\tanh\left(\frac{x_{FW}}{L_{FW}}\right)\sinh\left(\frac{x_{BZ}+\delta-x_{FW}}{L_{BZ}}\right)}
\end{aligned} \tag{26}$$

4 Multi-group solution

To extend this model to account for reaction cross-section variation as neutron lethargy increases, one can replace the neutron spectrum $\phi(x)$ with a position-dependent vector $\boldsymbol{\phi}(x)$. Here, we assume the emitted neutrons are monoenergetic, produced at the maximum energy of 14.06MeV. Analysing $\phi_1(x)$ would give the same result as Equation 10. Since no other groups can scatter neutrons into it, group 1's neutron flux is going to be of the same form that given by Equation 10. The only difference is that the constants D, L, δ in Equations 11, 12, 13, and 14 are swapped in for group 1's group-wise constants instead of the one-group constants used in Section 3.1.

Meanwhile, solving for higher lethargy neutron groups, we have:

$$D_2\frac{d^2}{dx^2}\phi_2(x) = (\Sigma_{t,2} - \Sigma_{s(2\to2)})\phi_2(x) - \Sigma_{s(1\to2)}\phi_1(x) \tag{27}$$

$$D_3\frac{d^2}{dx^2}\phi_3(x) = (\Sigma_{t,3} - \Sigma_{s(3\to3)})\phi_3(x) - \Sigma_{s(1\to3)}\phi_1(x) - \Sigma_{s(2\to3)}\phi_2(x) \tag{28}$$

$$D_4\frac{d^2}{dx^2}\phi_4(x) = (\Sigma_{t,4} - \Sigma_{s(4\to4)})\phi_4(x) - \Sigma_{s(1\to4)}\phi_1(x) - \Sigma_{s(2\to4)}\phi_2(x) - \Sigma_{s(3\to4)}\phi_3(x) \tag{29}$$

$$\vdots$$

Since the closed-form expression for ϕ_1, we deduce the closed-form expression for ϕ_2 with Equation 26; and therefore we can deduce the closed-form expression for ϕ_3 with Equation 27; and so on, until $\phi_i(x)\ \forall\ i$ are solved.

4.1 Solution by induction

Examining the differential Equations 26 to 28, one can see that it resembles the form of a driven (undamped) harmonic oscillator, but with a flipped sign. Solving for Equation 26 with a symbolic solver engine (WolframAlpha), where we set $\phi_1(x) = c_1 e^{\frac{|x|}{L_1}} + c_2 e^{-\frac{|x|}{L_1}}$, we have

$$\phi_2(x) = \frac{L_1^2 L_2^2}{L_1^2 - L_2^2}\frac{\Sigma_{s(1\to2)}}{D_2}\left(c_1 e^{\frac{|x|}{L_1}} + c_2 e^{-\frac{|x|}{L_1}}\right) + k_1 e^{\frac{|x|}{L_2}} + k_2 e^{-\frac{|x|}{L_2}} \,, \tag{30}$$

L_2 is given by extending definition 9 to get

$$L_i = \sqrt{\frac{D_i}{\Sigma_{t,i} - \Sigma s, (i \to i)}}\,,$$

$$D_i = \frac{1}{3(\Sigma_{t,i} - \frac{2}{3A}\Sigma_{s,(i\to i)})}\,,$$

k_1 and k_2 are integration constants to be determined by applying conditions.

As the neutron group number i increase, the closed-form expression will likely grow to be a superposition of $2i$ exponential functions, where the constants in front of the $e^{\frac{|x|}{L_i}}$ and the $e^{-\frac{|x|}{L_i}}$ term has to be determined by boundary conditions.

4.1.1 Boundary conditions

The solution ϕ_2 must be a piecewise solution, splitting at x_{FW}.

$$\phi_{2,FW}(x) = \frac{L_{FW,1}^2 L_{FW,2}^2}{L_{FW,1}^2 - L_{FW,2}^2}\frac{\Sigma_{s,FW(1\to2)}}{D_{FW,2}}\left(c_1 e^{\frac{|x|}{L_{FW,1}}} + c_2 e^{-\frac{|x|}{L_{FW,1}}}\right) + c_5 e^{\frac{|x|}{L_{FW,2}}} + c_6 e^{-\frac{|x|}{L_{FW,2}}} \quad (31)$$

$$\phi_{2,BZ}(x) = \frac{L_{BZ,1}^2 L_{BZ,2}^2}{L_{BZ,1}^2 - L_{BZ,2}^2}\frac{\Sigma_{s,BZ(1\to2)}}{D_{BZ,2}}\left(c_3 e^{\frac{|x|}{L_{BZ,1}}} + c_4 e^{-\frac{|x|}{L_{BZ,1}}}\right) + c_7 e^{\frac{|x|}{L_{BZ,2}}} + c_8 e^{-\frac{|x|}{L_{BZ,2}}} \quad (32)$$

such that

$$\phi_2(x) = \begin{cases} \phi_{2,FW}(x) & \text{when} \quad 0 < |x| \le x_{FW}\,, \\ \phi_{2,BZ}(x) & \text{when } x_{FW} < |x| \le x_{BZ} + \delta\,. \end{cases} \quad (33)$$

c_1 to c_4 have been defined in Section 3.1; and c_5 to c_8 will be determined by the boundary conditions below.

With the exception of condition 11, three of the four boundary conditions used in Section 3.1 can be modified to apply here.

- Flux continuity at the first-wall-blanket interface,

$$\phi_{2,FW}(x_{FW}) = \phi_{2,BZ}(x_{FW})\,. \quad (34)$$

- Neutron current density equality on either side of the first-wall-blanket interface,

$$D_{FW,2}\frac{d}{dx}\phi_{2,FW}(x)\bigg|_{x_{FW}} = D_{BZ,2}\frac{d}{dx}\phi_{2,BZ}(x)\bigg|_{x_{FW}}\,. \quad (35)$$

- Zero flux at the extended boundary, i.e.

$$\phi_{2,BZ}(x_{BZ} + \delta) = 0 \quad (36)$$

  - Where the δ is calculated by

$$\delta = 0.7104 \times 3D_{BZ,2}$$

And finally, in place of condition 11, a different condition about the total available neutron flux has to be added to fully determine the values of c_5 to c_8:

- In a steady state, the total number of neutrons entering group 2 should be the same as the number of neutrons leaving group 2, i.e. In-scatter from group 1 to group 2 = reactions removing neutrons from group 2 + escaped group 2 neutrons.

$$\underbrace{\int_{x>0}^{x=x_{BZ}} \Sigma_{s(1\to 2)}\phi_1(x)dx}_{\text{In-scatter}} = \underbrace{\int_{x>0}^{x=x_{BZ}} (\Sigma_{t,2} - \Sigma_{s,(2\to 2)})\phi_2(x)dx}_{\text{neutron-removing reactions}} + \underbrace{\left(-D_{BZ,2}\frac{d}{dx}\phi_2(x)\bigg|_{x_{BZ}}\right)}_{\text{escaped neutrons}} \tag{37}$$

Considering the complicated boundary conditions listed in Section 4.1.1, especially how the complexity of Equation 36 will increase rapidly with every new group added, we think it will be difficult to determine the integration constants c_5, c_6, ... etc. Therefore significant time would be required to derive a closed-form solution to the multi-group equation, via induction/recursion relation or otherwise.

We think generalizing the one-group solution to a multi-group solution will only have minimal impact on our target quantity (neutron heating in the first wall, blanket, and neutron lost), acting as higher order correction terms that only provide marginal improvements to the accuracy of the solution to an already oversimplified model. We therefore decide to terminate the study here, and do not derive the closed-form multi-group solution. As long as the first wall and blanket are not made of materials with large neutron-capture resonance peaks, the one-group solution provided by Section 3 should suffice.

For the keen reader who wishes to still implement a solver that finds the exact integration constants (without explicitly solving the boundary conditions 33 to 36), they can simply do so using off-the-shelf optimizers. This optimization may be more tractable to solve than directly solving the PDE in Equation 26 to 28. However, those who proceed with this optimization approach are advised to ensure strict convergence to avoid accumulating errors in the integration constants, as the higher lethargy neutron group's integration constants will be solved using equations involving lower lethargy neutron groups' integration constants.

References

[1] James J Duderstadt and Louis J Hamilton. Nuclear reactor analysis. John Wiley & Sons, Editorial: New York, 1976.